



25th International Congress of Theoretical and Applied Mechanics

August 22-27, 2021

BOOK OF ABSTRACTS

Editor: Alberto Corigliano

ISBN number: 978 -83-65550-31-6

under the auspices of



**POLITECNICO
MILANO 1863**



**UNIVERSITÀ
DI PAVIA**

www.ictam2020.org



ICTAM
Milano 2020+1
Virtual

ELASTIC RINGS SEDIMENTING IN A VISCOUS FLUID

Magdalena Gruzziel-Słomka¹, Paweł Kondratiuk², Piotr Szymczak², and Maria L. Ekiel-Jeżewska*¹

¹Institute of Fundamental Technological Research, Polish Academy of Sciences, Pawińskiego 5B, 02-106, Warsaw, Poland

²Institute of Theoretical Physics, Faculty of Physics, University of Warsaw, 02-093, Pasteura 5, Warsaw, Poland

Summary Dynamics of elastic rings settling under gravity at low-Reynolds-number are analyzed numerically. The bead model is used with Rotne-Prager-Yamakawa approximation of the hydrodynamic mobility matrix for the beads. Several attracting dynamical modes are found for a wide range of values of the elasto-gravitational number, and for many different initial configurations. The modes are stationary configurations, stationary shapes with the beads moving periodically along the ring, rotating rigid configurations or periodically changing shapes. Very stiff rings are circular and orient vertically. Less stiff ones tend to form almost circular and almost flat structures that are inclined with respect to gravity. Even more flexible rings deform significantly and reach one of several characteristic periodic orbits. Mean sedimentation velocities of different modes in general are different.

INTRODUCTION

Recently, there has been a lot of interest in topology and dynamics of deformable, closed, thin and long elastic chains (here called rings) moving in a viscous fluid. The motivation for developing theoretical models comes from biological systems such as DNA, proteins or ring polymers that spontaneously form similar structures [1, 2, 3]. Moreover, elastic rings can serve as simple models of vesicles, red blood cells [4], or swimming microorganisms, e.g., bacteria or algae [5]. Theoretical models of sedimenting elastic rings help to investigate the influence of gravity on the dynamics of microorganisms, to design new diagnostic tools in medicine and to apply ultracentrifugation to sort proteins or DNA.

SYSTEM AND ITS THEORETICAL MODEL

Here we focus on sedimentation of an elastic unknotted ring. We assume that the Reynolds number is much smaller than unity and that the Brownian motion is negligible. We report our recent results [6] on characteristic attracting dynamical modes and their shapes. Additionally, we evaluate and discuss the corresponding sedimentation speeds. An elastic ring is modeled as a chain of N overlapping identical spherical beads of diameter d . Centers of the consecutive beads are connected by springs of equilibrium length $l_0 = 0.6d$ and a large spring constant $50F_0/d$, where F_0 is a gravitational force, corrected for buoyancy, acting on each of the beads. The harmonic bending potential energy equals to $-\sum_{i=2}^{N-1} A^* \phi_i^2 / (2l_0)$, where ϕ_i is the angle between the springs attached to the bead i , and A^* is the bending stiffness. A wide range of values of the stiffness ratio $\tilde{A} = 6 \times 10^4 \times A^* / (F_0 N^3 l_0^2)$ is studied, where $A^* / (F_0 N^3 l_0^2)$ is the inverse elasto-gravitational number. To prevent a chain self-crossing, Lennard-Jones potential energies $\epsilon[(\sigma/r_{ij})^{12} - (\sigma/r_{ij})^6]$ are summed up over non-consecutive beads i, j with center-to-center distances $r_{ij} < 2^{1/6}\sigma$, where $\sigma = d/2$ and $\epsilon = dF_0/4$.

The dynamics is based on the Stokes equations. The motion of center \mathbf{r}_i of bead i satisfies $\dot{\mathbf{r}}_i = \sum_{j=1}^N \boldsymbol{\mu}_{ij} \cdot \mathbf{F}_j$, with the force \mathbf{F}_j determined from the sum of the spring, bending and Lennard-Jones potential energies presented above, plus the gravitational force (corrected for buoyancy), $\mathbf{F}_g = (0, 0, F_0)$. We adopt the Rotne-Prager-Yamakawa approximation for the mobility matrix $\boldsymbol{\mu}_{ij}$ [7] and solve the dynamics numerically.

RESULTS

Initially horizontal circle remains circular and horizontal while sedimenting. Therefore, we start our analysis from evaluating evolution of elastic rings that initially form flat circular rings in elastic equilibria, slightly inclined with respect to the horizontal plane. We observe that an elastic ring tends to one of several attracting orbits, depending on the stiffness ratio \tilde{A} . Rings with a large stiffness ratio \tilde{A} after a long time become *vertical* and remain circular. When \tilde{A} decreases, the final stationary shapes become more and more *tilted* from vertical, and deviations from circular and planar shape increase. Then, for even more flexible rings, other attracting modes are observed. In the *swinging* and *flapping* modes, the ring shape changes periodically with time, as illustrated in Fig. 1. One of shapes from each sequence in Fig. 1 is also

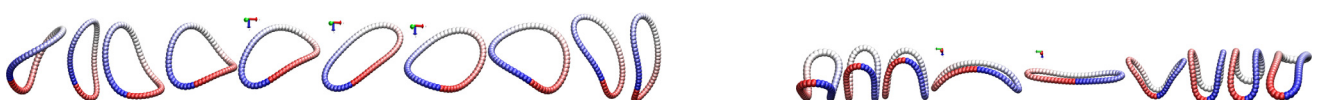


Figure 1: Snapshots from the swinging (left) and flapping (right) modes [6]. Gravity points down.

*Corresponding author. E-mail: mekiel@ippt.pan.pl

shown in Fig. 2a where names of all the modes are associated with certain characteristic shapes. In the *frozen rotating* and *figure eight* modes, the rigid shapes, shown in Fig. 2a, rotate around vertical axis. In the *tank-treading* mode, the beads move periodically along the configuration shown in Fig. 2a. In the *toroidal* modes with *two* or *three coils* ($T_{2,1}$ or $T_{3,1}$), the beads swirl in the poloidal direction and rotate in the toroidal direction, i.e., around vertical axis. In Fig. 2a, we also demonstrate that for the chosen class of the initial configurations, the smaller \tilde{A} , the more compact is the ring, with the smaller radius \tilde{R}_g of gyration (evaluated with respect to the center-of mass), averaged over many periods. Here $R_0 = Nl_0/(2\pi)$ is the radius of the initially circular and inclined ring.

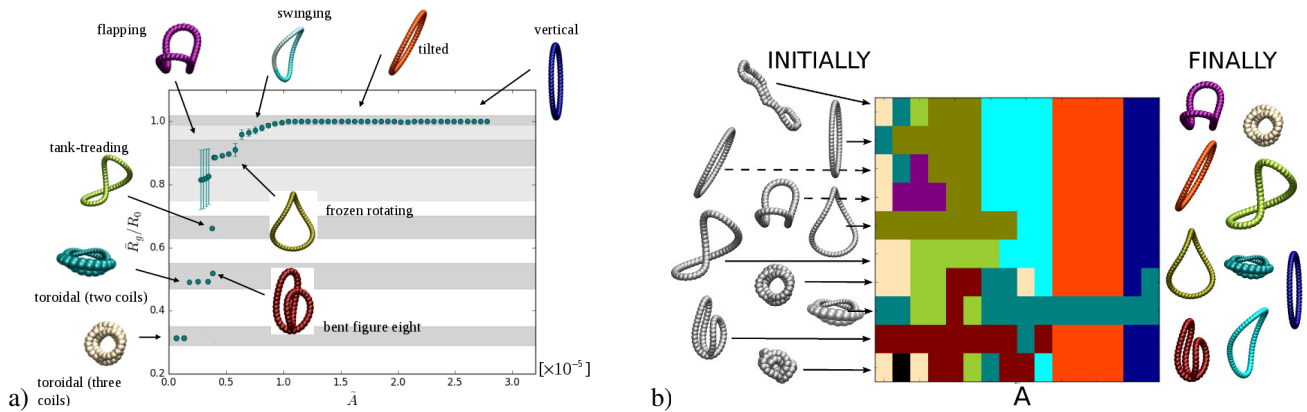


Figure 2: Shapes of sedimenting elastic rings, characteristic for different attracting dynamical modes with $N = 60$ and different values of the stiffness ratio \tilde{A} [6]. Gravity points down except the toroidal, three coils mode for which it points towards the reader. The initial configurations are: a) flat circular ring in elastic equilibrium, inclined by $\beta_0 = 16^\circ$ to the horizontal plane; b) characteristic shapes from the attracting dynamical modes, shown in panel a). In panel b), $\tilde{A} \in [0.23, 2.37]$, with a nonlinear scale shown in Fig. 20 of Ref. [6].

In Fig. 2b, we present simulations performed for another family of initial conditions. Each row in Fig. 2b corresponds to an initial configuration (indicated by arrow), that appeared in a different long-time dynamical mode shown in Fig. 2a. The colors correspond to the final stages of the evolution, shown at the right. The initial configuration in the last row and black color of the final stage correspond to an irregular coil.

The results shown in Fig. 2 illustrate very rich dynamics of sedimenting elastic loops. We have found many different attracting dynamical modes for the stiffness ratio $0.1 \leq \tilde{A} \leq 2.5$. Moreover, for a given value of \tilde{A} , different modes can emerge from different initial configurations. To complete the analysis performed in Ref. [6], we have also evaluated and analyzed sedimentation speeds of elastic loops in different modes, and for different values of \tilde{A} . Shapes, gyration radii and sedimentation velocities of elastic rings from the same mode only weakly depend on the stiffness ratio \tilde{A} , but in general they are significantly different for different dynamical modes observed for the same value of \tilde{A} . For example, as shown in Fig. 2b, a very compact shape of the toroidal mode with two coils has been observed in a wide range of the stiffness ratio, coexisting with almost circular vertical and tilted modes for $\tilde{A} \geq 1.22$. A more compact toroidal mode with three coils has been also detected for larger values of \tilde{A} . As the result, for a larger value of \tilde{A} , gyration radii and sedimentation velocities of different modes can differ even as much as by a factor of 3 and 2, respectively.

We analyzed dynamics of elastic loops made of different numbers of beads N . For $N > 15$, elastic rings behave similarly in similar ranges of the stiffness ratio \tilde{A} , i.e., in similar ranges of the elasto-gravitational number. This finding indicates that the attracting dynamical modes described here are generic for dynamics of very elastic sedimenting rings.

ACKNOWLEDGMENTS

M. G.-S. and P. S. were supported in part by Narodowe Centrum Nauki under grant 2015/19/D/ST8/03199. The VMD package [8] was used to visualize shapes.

References

- [1] Stasiak A., Katritch V., Bednar J., Michoud D. and Dubochet J. Electrophoretic mobility of DNA knots. *Nature* **384**, 122, 1996.
- [2] Ercolini E., Valle F., Adamcik J., Witz G., Metzler R., Rios P. D. L., Roca J. and Dietler G. Fractal Dimension and Localization of DNA Knots. *Phys. Rev. Lett.* **98**: 058102, 2007.
- [3] Poier P., Likos C. N., Moreno A. J. and Blaak R. An Anisotropic Effective Model for the Simulation of Semiflexible Ring Polymers. *Macromolecules* **48**: 4983-4997, 2015.
- [4] Jay A. W. L. and Canham P. B. Sedimentation of single human red blood cells. Differences between normal and glutaraldehyde fixed cells. *J. Cell. Physiol.* **80**, 367372, 1972.
- [5] Rizvi M. S., Farutin A. and Misbah C. Three-bead steering microswimmers. *Phys. Rev. E* **97**: 023102, 2018.
- [6] Gruzziel-Słomka M., Kondratiuk P., Szymczak P. and Ekiel-Jeżewska M. L. Stokesian dynamics of sedimenting elastic rings. *Soft Matter* **15**: 7262-7274, 2019.
- [7] Rotne J. and Prager S. Variational treatment of hydrodynamic interaction in polymers. *J. Chem. Phys.* **50**, 48314837, 1969.
- [8] Humphrey W., Dalke A. and Schulten K. VMD: visual molecular dynamics. *J. Mol. Graphics* **14**: 33-38, 1996.